A Comparison of Phase Organization of Model Segmented Polyurethanes with Different Intersegment Compatibilities

9 AUTHORS, INCLUDING:

Rebeca Hernandez
Spanish National Research Council
50 PUBLICATIONS **709** CITATIONS

SEE PROFILE

Ajay Padsalgikar
St. Jude Medical
29 PUBLICATIONS **415** CITATIONS

SEE PROFILE

Microstructural Organization of Three-Phase Polydimethylsiloxane-Based Segmented Polyurethanes

Rebeca Hernandez,[†] Jadwiga Weksler,[‡] Ajay Padsalgikar,[‡] and James Runt*,[†]

Department of Materials Science and Engineering and Materials Research Institute, The Pennsylvania State University, University Park, Pennsylvania 16802, and AorTech Biomaterials, Dalmore Drive, Caribbean Park, Scoresby, Victoria 3179, Australia

ABSTRACT: Microphase separation is investigated for segmented polyurethane copolymers synthesized from 4,4′-methylenediphenyl diisocyanate and 1,4-butanediol as the hard segments and poly(hexamethylene oxide diol) and hydroxyl-terminated polydimethylsiloxane as soft segments. The neat PDMS-based diol exhibits two segmental relaxations corresponding to the principal repeating unit, $Si(CH_3)_2O$, and to the hydroxyl end-group segments. When incorporated in the polyurethanes, the siloxane units form their own phase, while the end-group segments are mixed with the second macrodiol and some short hard segment sequences. This is demonstrated by the results of dynamic mechanical analysis and wide-angle X-ray diffraction experiments. The microdomain morphology was characterized principally by small-angle X-ray scattering, and the scattering data were analyzed with a pseudo-two-phase model as well as a modified three-phase core−shell model.

I. Introduction

Segmented polyurethanes (PU) block copolymers are used frequently in cardiac surgery, most notably as intraaortic balloons, as the blood-contacting portion of blood pumps in "bridging" cardiac assist devices, catheters, and as a component of pacemaker leads.[1] The main concern associated with their long-term use in such biomedical devices is their susceptibility to chemical degradation (i.e., oxidation and hydrolysis).[2,3] Polyether-based thermoplastic polyurethanes were the first to be used in these applications; however, it is well-known that they are susceptible to degradation by oxidation. The degradation mechanism is thought to begin with the abstraction of the α-methylene hydrogen from the soft segment in the presence of a reactive oxygen species, followed by esterification of the radical intermediate via oxidation, and finally chain scission and/or chemical cross-linking via acid hydrolysis.[4] This has encouraged the search for new soft segment chemistries that would be more resistant to the biological milieu. Aliphatic polycarbonate soft segment polyurethanes have recently received much attention because of its superior oxidative biostability: the "pseudo"-π-electron system of the carbonate linkage has been proposed to impart chemical stability to this family of copolymers. However, they are prone to enzymatic hydrolytic degradation.[5,6] Another alternative is the introduction of polydimethylsiloxane soft segments. Polydimethylsiloxane-based PUs have been found to have good oxidative stability and good blood contacting properties.[7−9]

The introduction of nonpolar macrodiols such as polyisobutylene,[10,11] polybutadiene,[12,13] and polydimethylsiloxane[14−19] into the polyurethane backbone has been demonstrated to be difficult, due to the difference in solubility with conventional urethane components (i.e., diisocynates, diol, and diamine chain extenders). The first attempts in synthesizing PDMS-based polyurethanes resulted in materials with poor mechanical properties, attributed to the resulting low molecular weight and also to the absence of intersegment hydrogen bonding between

Table 1. Molecular Weights of Series I and II Copolymers

	M_n (g/mol)	M_w/M_n
Series I		
PU80-30	139 000	2.1
PU80-32.5	168 000	1.7
PU80-35	105 000	2.2
PU80-40	171 000	1.6
PU80-45	124 000	1.7
PU80-52	143 000	1.6
Series II		
PU80-40	171 000	1.6
PU98-40	158 000	1.7

PDMS and the hard segments.[20] In order to overcome this, a second soft segment macrodiol can be added to interject an intermediate polarity chemical species between the hard and PDMS soft segments. Studies carried out on such segmented copolymers synthesized from amino-terminated PDMS and poly(tetramethylene oxide) (PTMO) reported a multiphase structure: the PDMS was found to microphase separate from both the PTMO and the hard segments.[18] Previous studies carried out on polyurethanes synthesized from poly(hexamethylene oxide) (PHMO) and hydroxy-terminated PDMS reached similar conclusions.[21,22]

It has also been reported that terminal units attached to the ends of siloxane oligomers may act as a "compatibilizer" between the highly apolar PDMS and the polar hard segments.[17] It is well-known that when short copolymer end blocks are significantly different in composition from the polymer backbone, they tend to phase separate.[23] This effect can be exploited to modify polymer/polymer interfaces in immiscible blends. For example, in blends of polybutadiene and polydimethylsiloxane,[24] the interfacial tension is reduced by as much as 30% for blends containing amine-terminated PDMS. This is attributed to changes in the bulk morphology and explained by considering the end-group-modified PDMS as a random copolymer of PDMS and end-group segments.

In the case of segmented PU block copolymers, the influence of amino end groups on the properties and morphology of PDMS-based materials has been found to be larger for lower PDMS molecular weights.[18] In addition, in a comprehensive

[†] The Pennsylvania State University.
[‡] AorTech Biomaterials.

Polyhexamethylenoxide

α,ω- PDMS

1. PDMS/PHMO (80/20) mixture

2. Molten MDI-Prepolymer formation
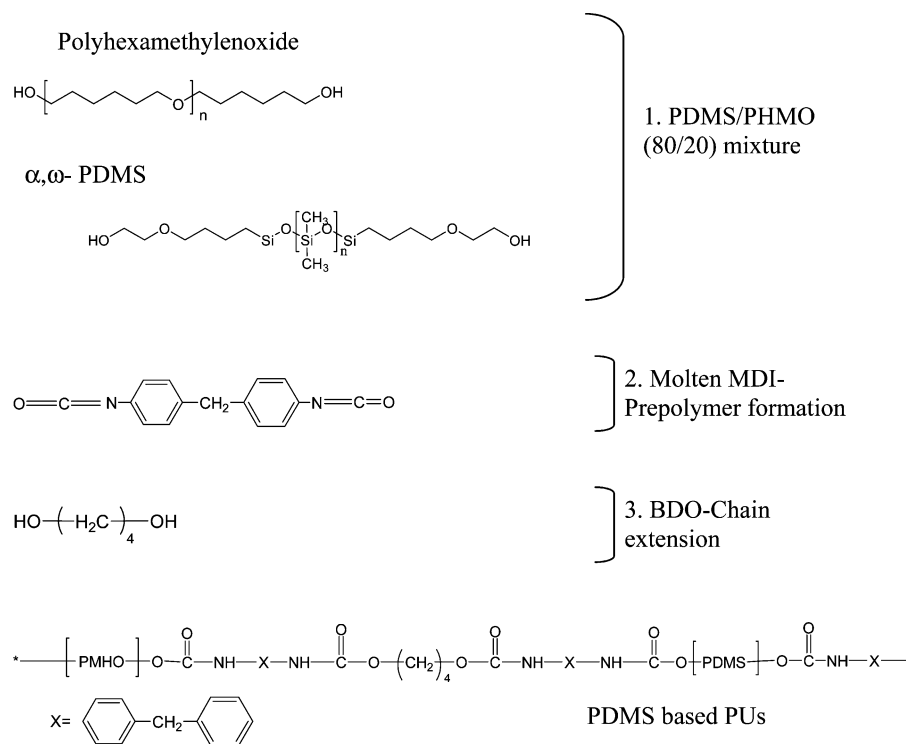
3. BDO-Chain extension

PDMS based PUs

Figure 1. Schematic representation of the synthesis.

small-angle X-ray scattering (SAXS) investigation of siloxane urea segmented block copolymers,[25] the authors noted that propyl units attached to the ends of the siloxane blocks may form intermediate regions between hard segments (composed of MDI without chain extension) and the siloxane blocks. This system was nevertheless treated as a two-phase system for the purposes of calculating the degree of phase separation, and values around 1 (i.e., complete segregation) were reported for PDMS molecular weights between 900 and 3960. The authors also found that the interfacial boundary in these materials was relatively small. These findings are in agreement with several other structural studies performed on siloxane polyurethanes that demonstrate that these materials are highly phase separated.[20,26]

In a continuation of our efforts to quantitatively investigate unlike segment demixing and corresponding properties in

segmented PUs of interest in biomedical applications (e.g., refs 27 and 28), we present a microstructural study of PU copolymers synthesized using mixed polyether and PDMS-based soft segments. We use SAXS as the principal experimental probe in this investigation and consider the influence of the two macrodiols, as well as terminal segments attached to PDMS, on the phase-separated structure.

II. Experimental Section

Materials. PU copolymers were synthesized[21] from 4,4′-methylenediphenyl diisocyanate (MDI) and 1,4-butanediol (BDO) as the hard segment and a mixture of macrodiols, α,ω-hydroxyl-terminated poly(dimethylsiloxane) (α,ω-PDMS) and poly(hexamethylene oxide), as the soft segments. The molecular weights of α,ω-PDMS and PHMO macrodiols are 1000 and 700 g/mol, respectively. A schematic representation of the synthesis is displayed in Figure 1. It should be noted that the copolymers were prepared by a two-step bulk polymerization method.

The first group of copolymers, referred to in this paper as series I, is composed of a mixture of α,ω-PDMS and PHMO (80/20 w/w) as the soft segments. The series I copolymers are identified by PU80 and a number denoting the hard segment weight fraction, calculated by including all MDI and BDO units to the hard segment. Samples with the following hard segment contents were synthesized (PU designation in parentheses): 30 wt % (PU80-30), 32.5 wt % (PU80-32.5), 35 wt % (PU80-35), 40 wt % (PU80-40), 45 wt % (PU80-45), and 52 wt % (PU80-52).

The copolymers in series II have the same hard segment weight fraction (40%) but vary in the stoichiometry of the soft segments. PU98-40 contains 98% α,ω-PDMS and 2% PHMO.

Gel Permeation Chromatography. All synthesized copolymers were characterized using gel permeation chromatography (GPC). The relative number-average molecular weights (M_n) and polydispersity indices (PDI) are shown in Table 1. The solvent used in the GPC experiments was DMF, and the reported molecular weights are relative to polystyrene standards. As expected, the PDIs $\sim$ 2, typical for polycondensation reactions. It is important to emphasize that the molecular weights of all materials are high, confirming the robustness of this procedure for synthesizing high molecular weight PDMS-containing segmented PUs.
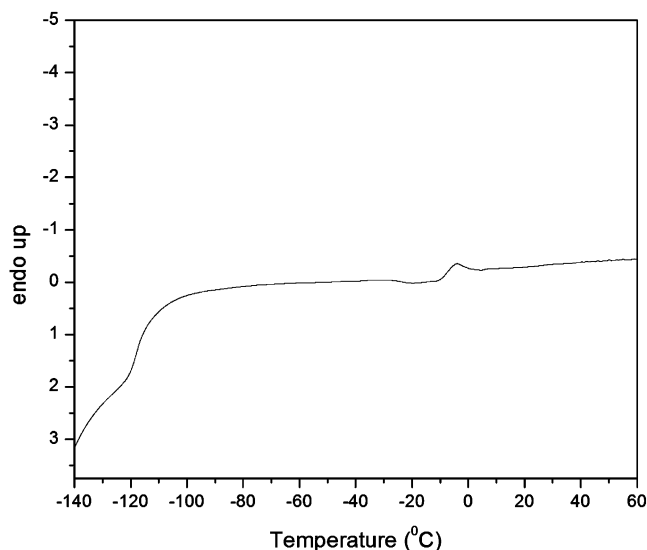

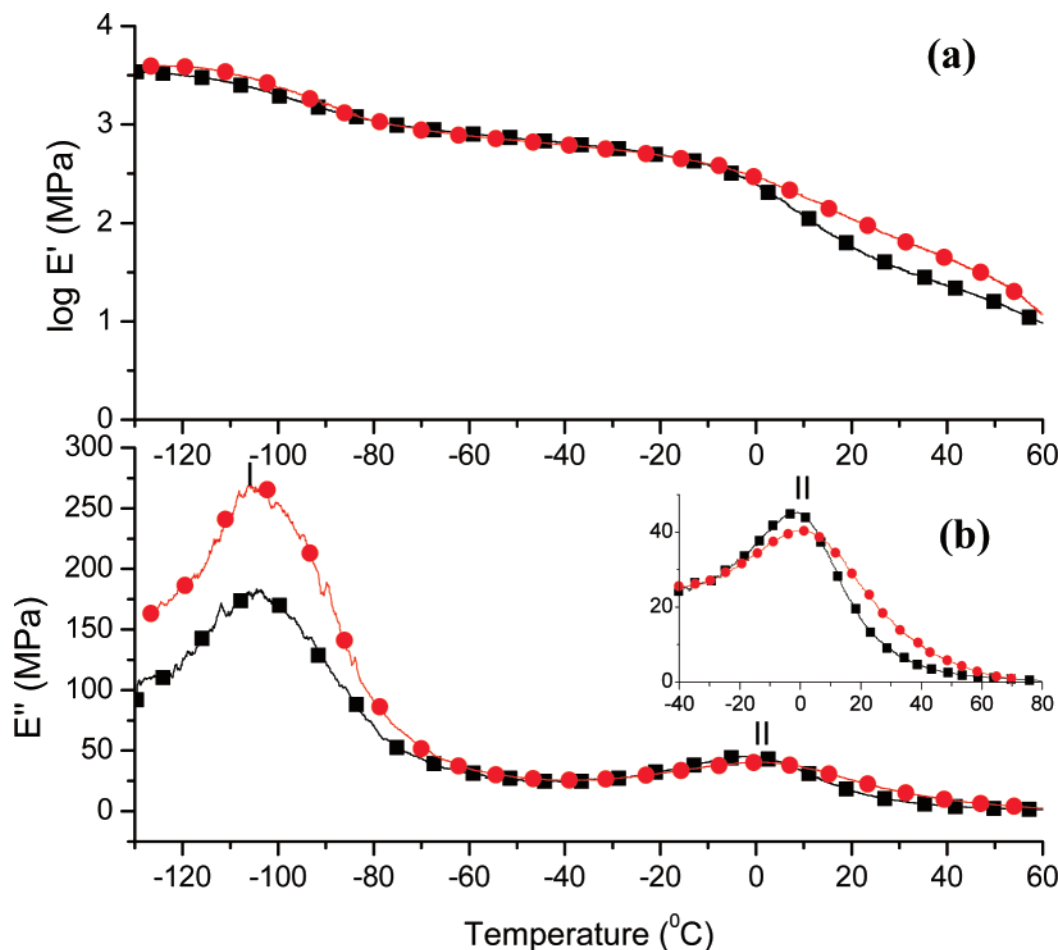**Figure 2.** DSC of neat α,ω-PDMS diol. Heating rate = 10 °C/min.

Figure 3. (a) Storage (E') and (b) loss moduli (E'') as a function of temperature for series II copolymers: ●, PU98-40; ■, PU80-40. Inset: ●, PU98-40; ■, PU80-40.

Dynamic Mechanical Analysis. The dynamic mechanical properties of the copolymers were evaluated using a TA-Q800 DMA and a gas cooling accessory (model CFL-50) for subambient experiments. Film samples were tested in tension from −120 to 150 °C at a heating rate of 3 °C/min and frequency of 1 Hz; the static force was preset at 1 N with a force track of 125%.

Wide-Angle X-ray Diffraction. These experiments were carried on a Scintag Pad V instrument using Cu Kα radiation ($\lambda = 0.154$ nm). The films were mounted on a quartz holder, and a scanning rate of 2°/min was used within the 2θ range of 3−40°.

Small-Angle X-ray Scattering. SAXS data were collected on Molecular Metrology SAXS instrument consisting of a three-pinhole collimated camera [using a Cu Kα radiation source ($\lambda = 0.154$ nm)] and a two-dimensional multiwire detector. The sample-to-detector distance was 1.5 m.

The PU films were cut into 1 cm × 1 cm squares, which were stacked to a thickness of ∼1 mm and secured by tape along the edges. The film stack was supported by placing it between two index cards with a hole for the passage of the X-ray beam. The ensemble was then mounted onto a sample holder provided by Molecular Metrology.

Absolute scattered intensities (in units of cm^{-1}) were determined by calibration with a precalibrated cross-linked polyethylene (S-2907) secondary standard; this step is essential in order to obtain quantitative details on segment demixing.[29] A silver behenate secondary standard was used to calibrate the scattering vector.

Integration of the scattering peak was conducted between the instrumental limits of q (0.07−1.7 nm^{-1}). Q values determined in this way are within 5% (and hence within experimental uncertainty) of those determined by integrating to infinite q (requiring extrapolation of the experimental high q scattering).

III. Results and Discussion

DSC experiments performed on the neat α,ω-PDMS macrodiol (Figure 2) reveal the presence of two T_gs, at −105 and −8 °C. The lower temperature transition can be reasonably assigned to the principal segments of α,ω-PDMS, $(Si(CH_3)_2O)_n$, and the second to the end-group segments that, due to significant differences in chemical structure (i.e., solubility parameters) with PDMS, are segregated and form their own phase. Similar results and interpretation have been reported for PDMS with amino end groups.[30]

Similarly, for the series II copolymers, the lowest temperature mechanical loss process, labeled as I and located at −105 °C at 1 Hz (Figure 3b), is assigned to the segmental motion of PDMS units. In addition, the strength of this relaxation scales with the α,ω-PDMS content, supporting this assignment. The location of this process does not change on the introduction of PHMO to the chain structure, indicating no discernible mixing between the siloxane units and PHMO (nor likely between the siloxane units and segments from the hard blocks) and the formation of microphases composed of only the PDMS repeating unit.

For PU98-40, the higher temperature segmental loss process (labeled as II and located at 2 °C at 1 Hz) is assigned to the α,ω-PDMS end-group segments, by comparison with the higher temperature T_g observed for the α,ω-PDMS macrodiol. The corresponding loss peak II shifts to 6 °C in the case of PU80-40 (see the inset in Figure 3b). We propose that this is a result of the mixing of the PDMS end-group segments with the PHMO, since the DSC T_g of the neat PHMO macrodiol was
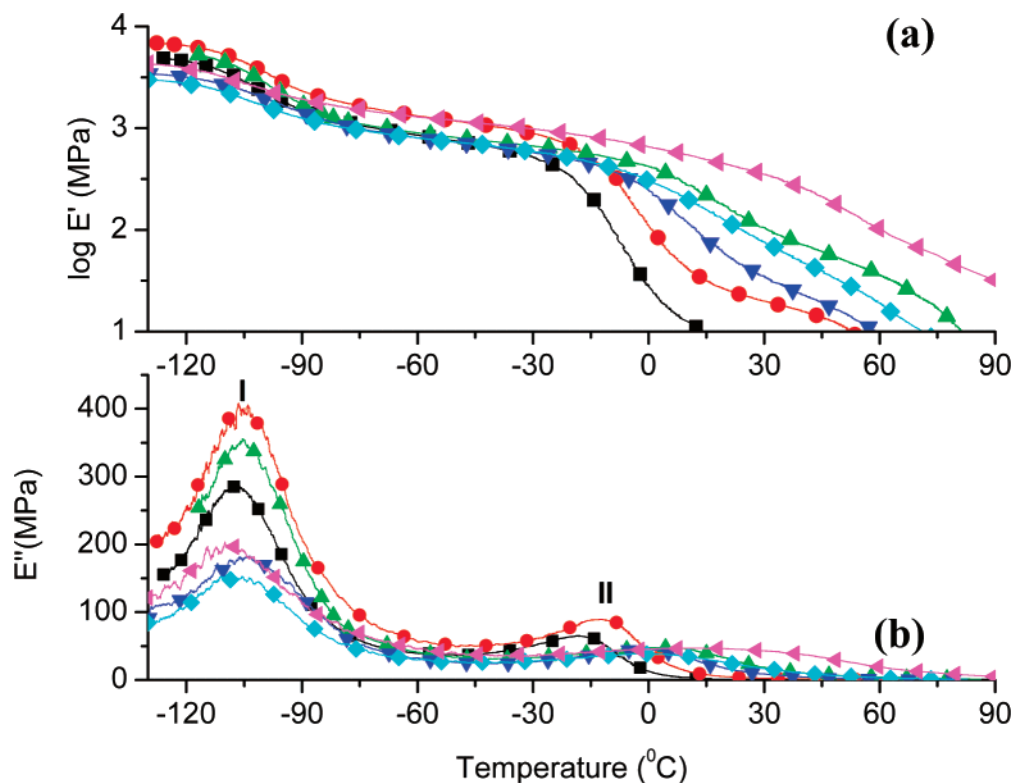
Figure 4. (a) Storage (E') and (b) loss moduli (E'') as a function of temperature for series I copolymers: ■, PU80-30; ●, PU80-32.5; ▲, PU80-35; ▼, PU80-40; ◆, PU80-45; tilted ▲, PU80-52.

found to be −35 °C. Numerous results in the literature point to extensive mixing of polyether soft segments with MDI−BDO hard segments[31] and even with MDI−ethylenediamine hard segments in polyurethane ureas.[28] Another factor influencing the position of the segmental relaxation II is the inclusion of "lone" MDIs (i.e., single MDI groups joining two soft segments in the absence of chain extender) and short MDI−BDO sequences into this phase.

The formation of a mixed phase composed of PHMO, PDMS end-group segments, and short hard segment sequences is more evident in the DMA results for the series I copolymers (Figure 4b). Segmental relaxation II broadens and moves to higher temperatures with increasing hard segment concentration, suggesting the inclusion of short MDI−BDO sequences into this phase. A similar finding has been reported by Cooper et al. and attributed to a greater fraction of hard segments dissolved in the soft phase.[32] This explanation is confirmed by the analysis of SAXS data of the copolymers under investigation here, as described in the following section. The formation of a phase composed at least predominately, perhaps entirely, of PDMS repeating units is confirmed for all series I compositions by the observation that the position of relaxation I does not change with hard segment concentration.

The corresponding storage modulus (E')−temperature behavior of the series I and II copolymers are shown in Figures 4a and 3a, respectively. The glassy state moduli for all copolymers are on the order of $10^{3.5}$ MPa, typical for polymer glasses. There is a reduction in E' as the copolymers pass through the α transition associated with the segmental motion in the siloxane phase. A second reduction in modulus coincides with the α transition associated with the predominately polyether phase. For copolymers with the same soft segment composition (series I) E' is a strong function of hard segment concentration in the temperature range between 25 and 37 °C. In this
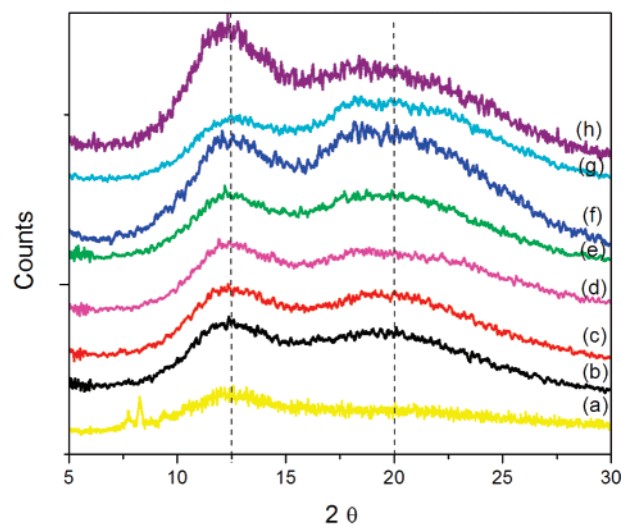

Figure 5. WAXD patterns for the copolymers: (a) α,ω-PDMS diol; (b) PU80-30; (c) PU-80-32.5; (d) PU80-35; (e) PU80-40; (f) PU80-45; (g) PU80-52; (h) PU98-40.

temperature range, PU98-40 presents a higher E' than PU80-40.

Figure 5 displays the WAXD patterns for all the samples. Neat α,ω-PDMS diol is noncrystalline and displays a characteristic amorphous halo at $2\theta = 12.5°$. The position of the α,ω-PDMS amorphous halo does not change in the copolymers, confirming the formation of a relatively pure PDMS phase. The second broad peak centered at $2\theta = 20°$ is typical of segmented PUs and poly(urethane urea)s and is indicative of the mean distance between non-PDMS segments. Note also the absence of diffraction peaks associated with 3D crystalline order for all copolymers under investigation here.
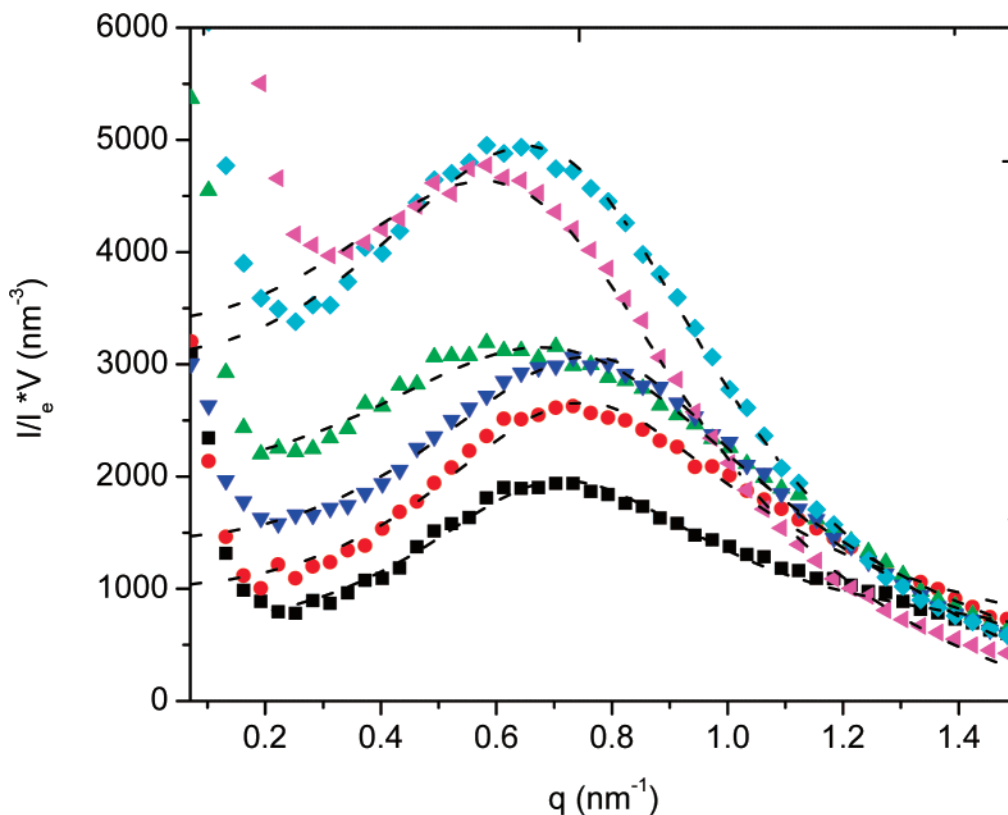
Figure 6. Background-corrected SAXS intensities as a function of scattering vector for PU series I copolymers: ■, PU80-30; ●, PU80-32.5; ▲, PU80-35; ▼, PU80-40; ◆, PU80-45; tilted ▲, PU80-52. Black dotted lines: fit to the Y−C model. The complete SAXS data sets consist of 200 points for a detector resolution 512 × 512. For easier visualization, some points have been removed from the curves in this figure.
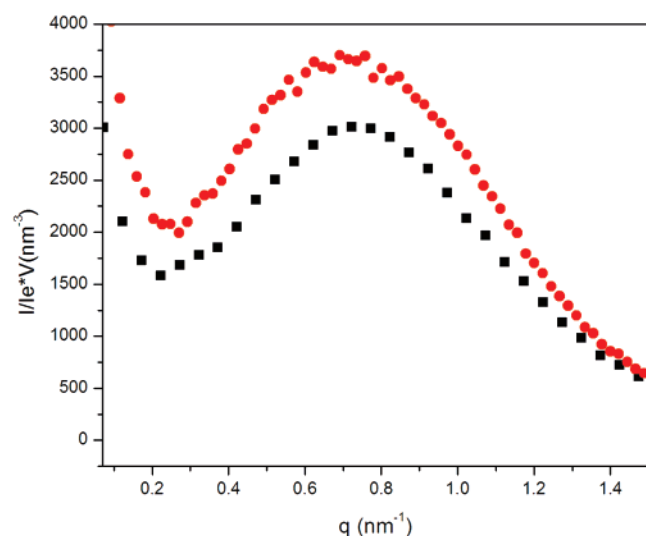

Figure 7. Background-corrected SAXS intensities as a function of scattering vector for series II copolymers: ■, PU80-40; ●, PU98-40. The complete SAXS data sets consist of 200 points. For easier visualization, some points have been removed from the curves in this figure.

Table 2. Mean Interdomain Spacings

	interdomain spacing/nm
Series I	
PU80-30	8.6
PU80-32.5	8.8
PU80-35	10.3
PU80-40	8.8
PU80-45	9.6
PU80-52	10.8
Series II	
PU80-40	8.8
PU98-40	8.6

Small-Angle X-ray Scattering. Experimental SAXS curves for the series I and II copolymers are displayed in Figures 6 and 7, respectively. The data are presented as $I/I_e V$, where I is the scattered intensity, I_e the intensity scattered by a single electron under identical conditions, and V the irradiated sample volume. The peak position (q_{max}) is indicative of the mean interdomain spacing, d, by $d = 2\pi/q_{max}$. Mean interdomain spacings are listed in Table 2. Except for PU80-35, d increases slightly with increasing hard segment content.

The models that are normally applied to two-phase segmented polyurethane SAXS data consider that the scattering peak results from the electron contrast between hard and soft phases.[33,34] In the case of three-phase systems like those under investigation here, one approach is to consider that one of the phases does not contribute significantly to the sample scattering, and thus its contribution can be included with one of the other two phases (i.e., as a pseudo-two-phase system[35]). Another alternative is to analyze the scattering using globular scattering models,[36] specifically a modified core−shell model that has been successfully applied to ionomers.[37,38] We apply both approaches to extract information about the microstructural organization of the series I and II copolymers.

Pseudo-Two-Phase Model. The DMA and WAXD results presented earlier support a three-phase microstructure for the α,ω-PDMS/PHMO PU copolymers: a phase composed of siloxane units (phase 1), hard domains (phase 2) that contain only hard segments, and a phase composed of PHMO, PDMS end-group segments, and (presumably short) hard segments (phase 3). Lone MDI units (i.e., MDIs that are not chain extended by BDO) are not expected to be associated with the hard domains and are located in phase 3.

Table 3. Theoretical Volume Fractions and Electron Densities for the *i*th Phases in the Copolymers under Consideration

	η_1 (mol e⁻/cm³)	ϕ_1	η_2 (mol e⁻/cm³)	ϕ_2	η_3 (mol e⁻/cm³)	ϕ_3	$\bar{\eta}$
			Series I				
PU80-30	0.570	0.56	0.734	0.22	0.634	0.22	0.614
PU80-32.5	0.570	0.56	0.733	0.24	0.635	0.19	0.619
PU80-35	0.570	0.54	0.732	0.26	0.635	0.20	0.623
PU80-40	0.570	0.54	0.730	0.30	0.635	0.15	0.630
PU80-45	0.570	0.48	0.727	0.35	0.635	0.17	0.635
PU80-52	0.570	0.51	0.724	0.39	0.635	0.09	0.643
			Series II				
PU80-40	0.570	0.54	0.730	0.3	0.635	0.26	0.630
PU98-40	0.570	0.56	0.730	0.3	0.610	0.14	0.624

The SAXS curves can be described in terms of an electron density variance. For a system with *n* phases, this variance is given by

$$\overline{\Delta\eta}^2 = \sum_i^n \phi_i(\bar{\eta} - \eta_i)^2 \qquad (1)$$

where $\bar{\eta}$ is the average electron density:

$$\overline{\Delta\eta} = \sum_i^n \phi_i\eta_i \qquad (2)$$

ϕ_i is the volume fraction and η_i the electron density of the *i*th phase defined as

$$\eta_i = \frac{\rho_i n}{M} \qquad (3)$$

where ρ_i is the mass density of the *i*th phase in g/cm³, *n* is the total number of electrons present in the structure, and *M* is the molecular weight.

From eq 1, it can be seen that when the electron density of a phase is equal to the average electron density, there is no contrast for this phase, and therefore it does not contribute to the observed scattering profile.[39] For calculation of the average electron density corresponding to each of the components/phases, the volume fraction, ϕ_i, for each was calculated by

$$\phi_i = \frac{W_t\rho_t}{\rho_i} \qquad (4)$$

W_t corresponds to the weight fraction of each phase, calculated taking into account the PDMS end group segments that constitute 20% of the total weight of the α,ω-PDMS diol. ρ_t is the overall copolymer density calculated following a group contribution method.[40] The density of the siloxane segments is 0.98 g/cm³. To account for the contribution of "lone" MDIs included in phase 3, the distribution of hard segment sequence lengths in the copolymers was computed by following the method of Peebles.[41] The hard phase was taken to include the remaining MDIs and BDOs. The density of neat MDI−BDO was calculated, following a group contribution method,[40] to be 1.33−1.40 g/cm³, in good agreement with the literature values for noncrystalline MDI−BD.[31]

The electron densities and volume fractions for each of the three phases having the noted "theoretical" compositions were calculated according to eqs 3 and 4. The average electron density for each composition in series I and II (calculated according to eq 2) are presented in Table 3. The calculations demonstrate that the electron density of phase 3 is comparable to the average value of the copolymer for series I samples with hard segment concentrations ≥40 wt %, and it is therefore a reasonable approximation to treat the system with a pseudo-two-phase

model for these cases. For compositions containing <40% hard segments and the sample 98-40, the definition of a pseudo-mixed phase is less clear.

The most general two-phase model for quantification of the degree of phase separation of polyurethanes and polyurethane ureas[28,31,42] is the Bonart and Mueller approach.[33,34] In this model, a theoretical variance is first calculated assuming complete phase separation of hard and the soft segments. In the systems under consideration here, this reduces to calculating the theoretical variance between a phase composed of siloxane units having a volume fraction ϕ_1 and electron density η_1 and a phase composed of the hard segments, PHMO, and PDMS end-group segments having a volume fraction ϕ_M and electron density η_M. The theoretical variance is then defined as

$$\overline{\Delta\eta_c}^2 = \{\phi_1(1 - \phi_1)(\eta_M - \eta_1)^2\} \qquad (5)$$

In order to determine whether it is reasonable to include the contribution of segments in phase 3 with phase 2, thus resulting in a hypothetical mixed phase, we calculate an invariant, Q^0, according to two different scenarios: *case A*: electron density contrast between phase 1 (siloxane units) and a second phase composed of mixed hard segments, PHMO, and PDMS end-group segments; *case B*: electron density contrast between siloxane units and a second phase composed of hard segments only. The general expression for Q^0 for a two-phase model is

$$Q^0 = 2\pi^2\{\phi_1(1 - \phi_1)(\eta_2^0 - \eta_1)^2\} \qquad (6)$$

The values are then compared with those obtained for a three-phase isotropic system in which the correlation function is expressed as a summation of the correlation functions of the individual phases $\gamma_i(r)$. For three-phase isotropic systems, the SAXS invariant can be expressed as[43,44]

$$Q = 2\pi^2\{\phi_1\phi_2(\eta_1 - \eta_2)^2 + \phi_2\phi_3(\eta_2 - \eta_3)^2 + \\ \phi_1\phi_3(\eta_1 - \eta_3)^2\} \quad (7)$$

Q calculated using eq 7 (and the parameters in Table 3) are then compared to those obtained from a pseudo-two-phase system, provided that both ϕ_1 and η_1 are the same in both the three- and pseudo-two-phase cases. The volume fraction corresponding to phase 3 can then be obtained from[44]

$$Q - Q^0\left(\frac{\eta_1 - \eta_2}{\eta_1 - \eta_2^0}\right)^2 = 2\pi^2[(\eta_1 - \eta_2)^2(\phi_1(1 - \phi_1)) - (\phi_1(1 - \\ \phi_1) - \phi_1\phi_3) + \phi_2\phi_3(\eta_2 - \eta)_3^2 + \phi_1\phi_3(\eta_1 - \eta_3)] \quad (8)$$

Table 4 presents values for ϕ_3 calculated from eq 7 for the two hypothetical cases. The calculations were done for series I copolymers with hard segment concentration ≥40% in which the pseudo-two-phase approach was determined to be reason-

Table 4. Volume Fractions for Phase 3 Calculated from Eq 7

series I	ϕ_3	$\phi_3{}^a$	$\phi_3{}^b$
PU80-40	0.15	0.12	0.35
PU80-45	0.17	0.13	0.34
PU80-52	0.09	0.12	0.26

[a] Case A, as defined in the text. [b] Case B.

Table 5. Electron Density Variances for PU Copolymers (Units of (mol e⁻/cm³)²)

series I	$\bar{\eta}_c{}^2 \times 10^3$	$\bar{\eta}^{2\prime} \times 10^3$	deg of microphase separation $(\bar{\eta}^{2\prime}/\bar{\eta}_c{}^2)$
PU80-40	2.30	2.24	0.97 ± 0.04
PU80-45	2.44	2.91	1.19 ± 0.17
PU80-52	2.62	2.59	0.99 ± 0.20

able. The stoichiometric values for ϕ_3 (contained in the first column of Table 4) are in very good agreement with the values obtained for case A for all of these, justifying the formulation of a hypothetical mixed phase (i.e., inclusion of phase 3 segments with those of phase 2).

In order to determine the degree of phase separation between the two phases, we compare the theoretical variance calculated using eq 5 with the experimental variance $\overline{\Delta\eta^{2\prime}}$. $\overline{\Delta\eta^{2\prime}}$ is related to the SAXS invariant, Q (the experimental total scattering intensity), by a constant, c:

$$\overline{\Delta\eta^{2\prime}} = cQ = c\int_0^\infty I(q)q^2\,\mathrm{d}q \tag{9}$$

where

$$c = \frac{1}{2\pi^2 i_e N_A{}^2} = 1.76 \times 10^{-24}\ \mathrm{mol^2/cm^2}$$

and i_e is Thompson's constant for the scattering from one electron (7.94×10^{-26} cm²) and N_A is Avogadro's number.

The ratio of the experimental variance (eq 9) to the theoretical variance, calculated using eq 5, $\overline{\Delta\eta^{2\prime}}/\Delta\eta_c{}^2$, provides a measure of the overall degree of phase separation. This ratio returns a value between 0 and 1, with unity indicating complete phase separation and infinitely sharp phase boundaries. $\overline{\Delta\eta^{2\prime}}$ is determined simply from the background-corrected SAXS intensities. It incorporates mixing in the microdomains as well as the influence of diffuse phase boundaries.

The electron density variances and degrees of microphase separation are shown in Table 5. Overall degrees of phase separation are around 1 for all compositions, confirming the formation of an all-PDMS phase and the suitability of this model to explain the experimental DMA and WAXD results.

B. Globular Scattering Model. In order to separate the contribution of phase 3 from that of phase 2 in the scattering patterns, we now consider a modified core–shell model extensively applied to interpretate the scattering patterns of ionomers (referred to as the Yarusso–Cooper (Y–C) model): [20,37,38,45]

$$I(q) = I_e(q)V\frac{1}{V_P}F^2(q)\frac{1}{1 + (8V_{ca}/V_p)\epsilon\Phi(2qR_{ca})} \tag{10}$$

where ϵ is a constant ~1, R_{ca} the radius of closest dispersed phase approach, $V_{ca} = 4/3\pi R_{ca}{}^3$, V_p the average sample volume per particle, and $F(q)$ the structure factor of the particle. For a sphere of constant density

$$F(q) = \Delta\eta_1 V_1 \Phi(qR_1) \tag{11}$$
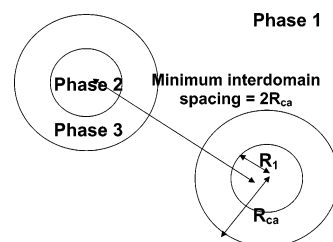
Figure 8. Schematic representation of the microphase-separated structure of of the PDMS-based polyurethanes, with parameters relevant to the Y–C noted.
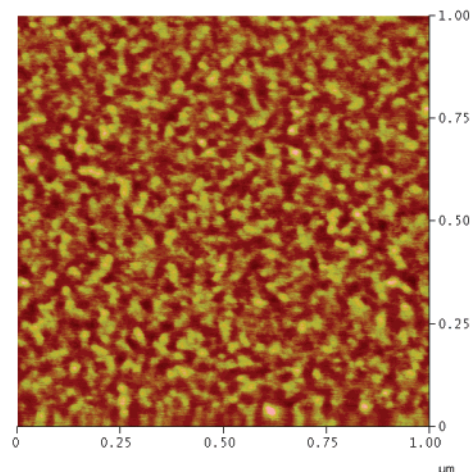
Figure 9. AFM tapping mode phase image of the as-received surface morphology of PU80-40. Image was obtained with a Digital Instruments with silicon probe in air. r_{sp} (set point amplitude/free amplitude of oscillation) = 0.2. Scale: 0–50. Image is 1 μm × 1 μm region.

where $\Delta\eta_1$ represents the difference in electron density between the core and the siloxane matrix and V_1 the volume of an spherical aggregate, $V_1 = 4/3\pi R_1{}^3$. $\Phi(x)$ is defined as

$$\Phi(x) = 3\frac{\sin x - x\cos x}{x^3} \tag{12}$$

A schematic drawing of a proposed core–shell model is provided in Figure 8. A core with radius R_1 represents the hard domains (phase 2) that are separated from the matrix (phase 1) by a region composed of PHMO and PDMS end-group segments ($R_{ca} - R_1$).

The use of a globular scattering model for segmented polyurethanes under consideration here is in keeping with AFM tapping mode phase images, an example of which is shown in Figure 9 (for PU80-40), in which hard domains appear as bright regions. It is possible to envision the series I copolymers as having a siloxane matrix in which spherical domains composed of hard segments, PHMO, and PDMS end-group segments are dispersed. As noted earlier, the formation of a completely separated phase composed of siloxane units is been confirmed by DMA and WAXD results presented earlier.

The dashed lines in Figure 6 show the fits of the globular model to the SAXS data in the q range between 0.4 and 1.5 nm⁻¹ for series I copolymers. The low angle intensity upturn at $q < 0.4$ nm⁻¹ that is evident in all SAXS patterns cannot be interpreted with the Y–C model. In the case of ionomers, ultra-small-angle X-ray scattering experiments have shown that this upturn is related to the distribution of ions on length scales on the order of 10–100 nm.[46,47] For the samples under consideration here, there are several possible explanations for the low q feature: the existence of aggregates with an interdomain spacing

Table 6. Best Fit Values Obtained from the Y−C Model

HS content	$\Delta\eta_1$ (nm^{-3})^b	$\Delta\eta_{HS}$ (nm^{-3})	$\Delta\eta_m$ (nm^{-3})	R_{ca} (nm)^b	R_1 (nm)^b	$V_p^{1/3}$ (nm)^b	V_1 (nm^3)	V_{HS} (nm^3)	Φ_{HS}
30	95^a	95	46	3.7	1.5	9.8	15	9	1
32	95^a	95	44	3.5	1.6	9.4	17	16	1
35	94^a	94	43	3.3	1.9	11.3	27	22	1
40	57	93	41	3.2	1.9	8.6	29		0.30
45	62	92	40	3.5	2.2	10.1	45		0.42
52	60	90	39	3.7	2.3	11.4	54		0.40

^{a} Fixed during regression. ^{b} Obtained from the regression.

beyond the measurement capabilities of the instrumentation used in this study or perhaps the improper subtraction of background scattering. The second possibility was discounted by the fact that the empty beam measurement was clean. Furthermore, other authors have likewise noted that, in the case of PUs, the background scattering contribution to low q intensities is negligible.[36,48]

For initial fitting purposes, $\Delta\eta_1$ was fixed as the difference in electron density between a hard segment core and siloxane matrix, and R_1, R_{ca}, and V_p were derived from the fitting.[38] A nonlinear least-squares regression was used to optimize the independent fitting parameters and generate the best-fit curves. The best fit parameters are summarized in Table 6. For hard segment concentrations of 35% and below, R_1 increases slightly with hard segment concentration. Mean hard domain diameters of 3−4 nm are obtained, and the core volume (V_1) is obtained from R_1. Assuming that the core is composed of hard segments without including lone MDIs, V_1 can be compared with the volume of the hard segment (V_{HS}) calculated from the stoichiometry of the sample. The volume occupied by the hard segment can be estimated using the density ($\rho_{HS} = 1.39 \times 10^{-21}$ g/nm^3) and molar mass of the hard segment without taking into account the lone MDIs. Using this method, V_{HS} can be calculated by the following expression:

$$V_{HS} = n_{HS}\left(\frac{M_{HS}}{N_a\rho_{HS}}\right) \tag{13}$$

where n_{HS} is the number of atoms in the hard domain. The values obtained are also provided in Table 6. There is a good agreement between V_1 and V_{HS}, thus confirming the validity of the model for describing the SAXS scattering from copolymers with hard segment concentrations <40%.

For copolymers with hard segment concentrations ≥40%, fixing $\Delta\eta_1$ as above did not result in an adequate fit of the data. Therefore, for the higher hard segment content materials, $\Delta\eta_1$ was allowed to vary within a physically reasonable range of values. The upper limit was set as the difference in electron density between the siloxane matrix and a core composed of hard segments only, $\Delta\eta_{HS}$; the lower limit was set as the difference in electron density between the siloxane matrix and a core composed of hard segments, PDMS end-group segments, and PHMO, $\Delta\eta_M$. The resulting $\Delta\eta_1$ are provided in Table 6— all values are between $\Delta\eta_{HS}$ and $\Delta\eta_M$. The volume fraction of hard segments, ϕ_{HS}, not involved in the mixed phase can be calculated using

$$\Delta\rho_1 = \phi_{HS}\Delta\eta_{HS} + (1 - \phi_{HS})\Delta\eta_m \tag{14}$$

For the copolymers with higher hard segment contents, results in Table 6 indicate that a relatively high volume fraction of hard segments are mixed with the polyether phase, and thus the scattering is a result of the interference between particles composed of hard segments, PHMO, and PDMS end-group segments. This result is in agreement with the conclusions

derived from the application of the pseudo-two-phase model in the previous section.

In all cases, R_{ca} is primarily affected by the position of the scattering peak, and the mean distance between hard domains is estimated as the cube root of the volume per aggregate.[49] The mean interdomain distance calculated from eq 1 lies between $2R_{ca}$ and $V_p^{1/3}$.

IV. Summary

The microstructural organization of PDMS-based polyurethanes synthesized from mixed macrodiols has been investigated. SAXS and other experimental findings support the formation of a siloxane phase without intermixing with the other soft segment components or the hard segments. The PDMS end-group segments are segregated and mixed with the polyether macrodiol, leading to a separate phase in which short hard segments can be dissolved. Therefore, the PUs under study organize into three phases: hard domains, siloxane domains, and a mixed phase composed of the second macrodiol, PDMS end-group segments, and dissolved hard segment sequences.

Two different approaches have been adopted to model the scattering from the three-phase system. In the first approach, a pseudo-two-phase model in which the scattering is the result of the contrast between the siloxane units and a phase composed of the hard segments, PHMO, and PDMS end-group segments is considered. This model is shown to be valid only for copolymers with hard segment concentrations ≥40 wt %.

The second approach is based on a modified hard-sphere scattering model. This model provides a good fit of the SAXS data for all samples that contain PDMS/PHMO (80/20 (w/w)) soft segments; however, the physical interpretation depends on the hard segment concentration.

For copolymers with hard segment concentrations less than 40 wt %, the model provides a good fit to the scattering data by assuming complete phase separation between the hard domains and the polyether phase. At hard segment concentrations ≥40 wt %, a high volume fraction of the hard segments are dissolved in the polyether phase. Thus, the inclusion of MDI−BDO sequences into the mixed phase increases with HS content, consistent with the location of the higher temperature DMA α process. For all compositions, the volume corresponding to the hard domains increases with hard segment concentration, and the obtained minimum interdomain spacing is in agreement with the results obtained from the position of the scattering peak.

References and Notes

(1) Lamba, N. M.; Woodhouse, K. A.; Cooper, S. L. *Polyurethanes in Biomedical Applications*; CRC Press: Boca Raton, FL, 1991.

(2) Anderson, J. M.; Hiltner, A.; Wiggins, M. J.; Schubert, M. A.; Collier, T. O.; Kao, W. J.; Mathur, A. B. *Polym. Int.* **1998**, *46*, 163.

(3) Pinchuk, L. *J. Biomed. Mater. Res.* **1994**, *6*, 225.

(4) Christenson, E. M.; Dadsetan, M.; Wiggins, M.; Anderson, J. M.; Hiltner, A. *J. Biomed. Mater. Res., Part A* **2004**, *69*, 407.

(5) Tang, Y. W.; Labow, R. S.; Santerre, J. P. *Biomaterials* **2003**, *24*, 2805.

(6) Labow, R. S.; Meek, E.; Santerre, J. P. *Biomaterials* **2001**, *22*, 3025.

(7) Simmons, A.; Hyvarinen, J.; Odell, R. A.; Martin, D. J.; Gunatillake, P. A.; Noble, K. R.; Poole-Warren, L. A. *Biomaterials* **2004**, *25*, 4887.

(8) Ward, R.; Anderson, J.; McVenes, R.; Stokes, K. *J. Biomed. Mater. Res.* **2006**, *77A*, 380.

(9) Ward, R.; Anderson, J.; McVenes, R.; Stokes, K. *J. Biomed. Mater. Res.* **2006**, *77A*, 580.

(10) Speckhard, T. A.; Strate, G. V.; Gibson, P. E.; Cooper, S. L. *Polym. Eng. Sci.* **1983**, *23*, 337.

(11) Speckhard, T. A.; Gibson, P. E.; Cooper, S. L.; Chang, V. S. C.; Kennedy, J. P. *Polymer* **1985**, *26*, 55.

(12) Chen-Tsai, C. H. Y.; Thomas, E. L.; MacKnight, W. J.; Schneider, N. S. *Polymer* **1986**, *27*, 659.

(13) Brunette, C. M.; Hsu, S. L.; Rossman, M.; MacKnight, W. J.; Schneider, N. S. *Polym. Eng. Sci.* **1981**, *21*, 668.

(14) Tyagi, D.; Wilkes, G. L.; Yilgor, I.; McGrath, J. E. *Polym. Bull. (Berlin)* **1982**, *8*, 543.

(15) Tyagi, D.; Yilgor, I.; McGrath, J. E.; Wilkes, G. L. *Polymer* **1984**, *25*, 1807.

(16) Yilgor, I.; Shaaban, A. K.; Steckle, W. P.; Tyagi, D.; Wilkes, G. L.; McGrath, J. E. *Polymer* **1984**, *25*, 1800.

(17) Yilgor, I.; McGrath, J. E. *Adv. Polym. Sci.* **1988**, *86*, 1.

(18) Sheth, J. P.; Aneja, A.; Wilkes, G. L.; Yilgor, E.; Atilla, G. E.; Yilgor, I.; Beyer, F. L. *Polymer* **2004**, *45*, 6919.

(19) Sheth, J. P.; Yilgor, E.; Erenturk, B.; Ozhalici, H.; Yilgor, I.; Wilkes, G. L. *Polymer* **2005**, *46*, 8185.

(20) Yu, X.-H.; Nagarajan, M. R.; Grasel, T. G.; Gibson, P. E.; Cooper, S. L. *J. Polym. Sci., Polym. Phys. Ed.* **1985**, *23*, 2319.

(21) Gunatillake, P. A.; Meijs, G. F.; McCarthy, S. J.; Adhikari, R. *J. Appl. Polym. Sci.* **2000**, *76*, 2026.

(22) Adhikari, R.; Gunatillake, P. A.; McCarthy, S. J.; Meijs, G. F. *J. Appl. Polym. Sci.* **2000**, *78*, 1071.

(23) Jalbert, C.; Koberstein, J. T.; Yilgoer, I.; Gallagher, P.; Krukonis, V. *Macromolecules* **1993**, *26*, 3069.

(24) Fleischer, C. A.; Koberstein, J. T.; Krukonis, V.; Wetmore, P. A. *Macromolecules* **1993**, *26*, 4172.

(25) Tyagi, D.; McGrath, J. E.; Wilkes, G. L. *Polym. Eng. Sci.* **1986**, *26*, 1371.

(26) Li, C.; Yu, X.; Speckhard, T. A.; Cooper, S. L. *J. Polym. Sci., Part B: Polym. Phys.* **1988**, *26*, 315.

(27) Garrett, J. T.; Lin, J. S.; Runt, J. *Macromolecules* **2002**, *35*, 161.

(28) Garrett, J. T.; Runt, J.; Lin, J. S. *Macromolecules* **2000**, *33*, 6353.

(29) Russell, T. P.; Lin, J. S.; Spooner, S.; Wignall, G. D. *J. Appl. Crystallogr.* **1988**, *21*, 629.

(30) Jalbert, C.; Koberstein, J. T.; Yilgor, I.; Gallagher, P.; Krunokis, V. *Macromolecules* **1993**, *26*, 3669.

(31) Leung, L. M.; Koberstein, J. T. *J. Polym. Sci., Polym. Phys. Ed.* **1985**, *23*, 1883.

(32) Cooper, S. L.; Miller, J. A.; Lin, S. B.; Hwang, K. K. S.; Wu, K. S.; Gibson, P. E. *Macromolecules* **1985**, *18*, 32.

(33) Bonart, R. *J. Macromol. Sci., Phys.* **1974**, *B10*, 345.

(34) Bonart, R. *J. Macromol. Sci., Phys.* **1974**, *B10*, 177.

(35) Koberstein, J. T.; Stein, R. S. *Polym. Eng. Sci.* **1983**, *24*, 293.

(36) Laity, P. R.; Taylor, J. E.; Wong, S. S.; Khunkamchoo, P.; Norris, K.; Cable, M.; Andrews, G. T.; Johnson, A. F.; Cameron, R. E. *Polymer* **2004**, *45*, 7273.

(37) Visser, S. A.; Cooper, S. L. *Macromolecules* **1991**, *24*, 2584.

(38) Yarusso, D. J.; Cooper, S. L. *Macromolecules* **1983**, *16*, 1871.

(39) Goodisman, J.; Brumberger, H. *J. Appl. Crystallogr.* **1971**, *4*, 347.

(40) Coleman, M. M.; Graf, J.; Painter, P. *Specific Interactions and the Miscibility of Polymer Blends*; Technomic Publishing: Lancaster, 1991.

(41) Peebles, L. H. *Macromolecules* **1976**, *9*, 58.

(42) Saiani, A.; Rochas, C.; Eeckhaut, G.; Daunch, W. A.; Leenslag, J. W.; Higgins, J. S. *Macromolecules* **2004**, *37*, 1411.

(43) Wu, W. *Polymer* **1982**, *23*, 1907.

(44) Marr, D. W. M.; Wartenberg, M.; Schwartz, K. B.; Agamalian, M. M.; Wignall, G. D. *Macromolecules* **1997**, *30*, 2120.

(45) Benetatos, N. M.; Chan, C. D.; Winey, K. I. *Macromolecules* **2007**, *40*, 1081.

(46) Wu, D. Q.; Chu, B.; Lundberg, R. D.; MacKnight, W. J. *Macromolecules* **1993**, *26*, 1000.

(47) Ding, Y. S.; Hubbard, S. R.; Hodgson, K. O.; Register, R. A.; Cooper, S. L. *Macromolecules* **1988**, *21*, 1698.

(48) Velankar, S.; Cooper, S. L. *Macromolecules* **1998**, *31*, 9181.

(49) Batra, A.; Cohen, C.; Kim, H.; Winey, K. I.; Ando, N.; Gruner, S. M. *Macromolecules* **2006**, *39*, 1630.